REDUCED-ORDER TRANSIENT SIMULATIONS OF THE CONVECTED WAVE EQUATION WITH PERFECTLY MATCHED LAYERS

Yinshan Cai[1,5*] **Gwénaël Gabard**[2] **Sjoerd van Ophem**[3]
Wim Desmet[1,5] **Elke Deckers**[4,5]
[1] Department of Mechanical Engineering, KU Leuven, Belgium
[2] Laboratoire d'Acoustique de l'Université du Mans (LAUM), UMR 6613,
Institut d'Acoustique - Graduate School (IA-GS), CNRS, Le Mans Université, France
[3] Institute of Sound and Vibration Research, University of Southampton, UK
[4] Department of Mechanical Engineering, KU Leuven, Campus Diepenbeek, Belgium
[5]Flanders Make@KU Leuven

ABSTRACT

Perfectly matched layers (PMLs) have been widely employed to create non-reflecting boundary conditions for various wave-propagation problems. Stability and efficiency are crucial for transient simulations of such systems. For wave propagation with flow, classical PMLs can suffer from stability issues. Although recent improvements address these concerns, we found they are inaccurate at low frequencies. In addition, PMLs require a sufficient number of layers to reduce numerical errors and result in additional variables in the time domain, leading to a high computational cost for transient simulations. This paper presents a novel reduced-order approach to enable fast, stable, and accurate transient simulations of the convected wave equation with PMLs. Firstly, the convected Helmholtz equation is transformed into a modified Helmholtz equation using the Lorentz transformation. The employment of PMLs in the Lorentz space guarantees stability and accuracy. Secondly, auxiliary variables are designed to build the time-domain model, where the stable model order reduction can be applied to accelerate the transient simulations. The proposed method is successfully verified by numerical experiments.

**Corresponding author*: *yinshan.cai@kuleuven.be.*

Keywords: *convected wave equation, perfectly matched layers, model order reduction, time domain, finite element method*

1. INTRODUCTION

The finite element method (FEM) has been widely employed for the solution of wave-propagation problems. However, it often results in large models for complex systems and higher excitation frequencies, because a sufficient mesh resolution needs to be applied to accurately represent the acoustic field. This hinders applications that require real-time transient simulations, such as virtual sensing that combines the FE model and limited measurements to infer the hard-to-measure variables [1]. Therefore, in the last decade, stability-preserving model order reduction (MOR) has been extensively studied to reduce the size of such FE models while retaining the high-fidelity and stability properties. They have been applied to wave-propagation problems in quiescent fluids, such as interior problems [1–3] and exterior problems [4].

In this paper, we focus on the exterior problems of wave propagation in a uniform mean flow, which can be described by the convected Helmholtz equation with non-reflecting boundary conditions. Perfectly matched layers (PMLs) have been introduced to mimic the non-reflecting boundary condition with a truncated computational domain and are extensively employed in various wave-propagation problems (e.g., the Helmholtz equation [4] and the linearized Euler equations [5]) due to their superior absorbing property independent of frequency and incident angle. However, PMLs are sometimes plagued by stability issues in the time domain. For the classical wave equation, i.e. with zero mean flow, the stability condition of PMLs is well studied in [6], showing that stability can be guaranteed by omitting the unstable term or using sufficiently thick PMLs. Recently, a stability-preserving MOR scheme based on such stability condition was proposed to preserve stability in the reduced-order model (ROM) and accelerate transient simulations [4]. However, the stability of PMLs for the convected wave equation is still an open topic, as is the stability-preserving MOR.

A contribution to the stability of PMLs for the convected Helmholtz equation was recently made by Marchner et al. [7], where the Lorentz transformation is applied to obtain a formulation with a structure similar to the Helmholtz equation. The authors indicate that applying the usual PMLs to this formulation can provide a stable model through a plane wave stability analysis in the frequency domain, which outperforms the existing PML techniques [8]. However, this cannot be generalized to all situations, such as a two-dimensional problem with the flow direction not parallel to the coordinate axis, as will be explained in Section 2 and 4.

In this work, a formulation of the convected wave equation with PMLs, together with the corresponding stability-preserving MOR, is proposed to accelerate the transient simulations. The paper is structured as follows. Section 2 shows the stable convected wave equation with PMLs. Then, in Section 3, the stability-preserving MOR scheme is explained. Numerical experiments are provided in Section 4 to verify stability and efficiency. Finally, conclusions are given in Section 5.

2. STABLE PMLS

The convected wave equation that represents the wave propagation in a background flow with stationary flow speed $\boldsymbol{v}_0 = (v_x, v_y)^T$ is expressed as:

$$\frac{D_0}{Dt}\left(\frac{1}{c_0^2}\frac{D_0\phi(t)}{Dt}\right) - \nabla_{\boldsymbol{x}}^2\phi(t) = f(t), \tag{1}$$

where $\frac{D_0}{Dt} = \frac{\partial}{\partial t} + \boldsymbol{v}_0 \cdot \nabla_{\boldsymbol{x}}$, $\boldsymbol{x} = (x, y)$ is the spatial variable in the physical space, t is the time variable, $\phi(t)$ is the acoustic potential in the physical space, and c_0 is the speed of sound. It is worth noting that in this paper the two-dimensional problem is considered for simplicity, but the extension to the three-dimensional case is also possible [9]. The instability of PMLs for wave propagation in moving medium is generally attributed to flow effects [5, 7, 8]. In [7], a combination of a Lorentz and Galilean transformation is applied to remove the presence of flow. It is defined by

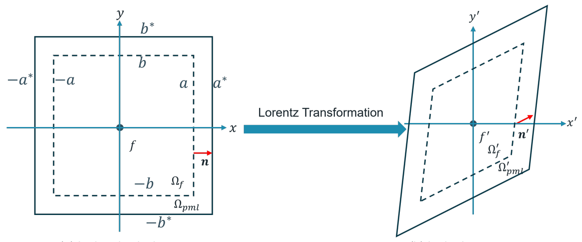

(a) In the physical space (b) In the Lorentz space

Figure 1. A 2D problem with a Mach number $M = \|\boldsymbol{M}\| = 0.8$ and an flow angle $\theta = \pi/4$, which is a rectangle in the physical space.

$$\begin{aligned} \boldsymbol{x}' &= \mathbf{L}\boldsymbol{x}, \\ t' &= \beta t + \frac{(\boldsymbol{M}\cdot\boldsymbol{x})}{\beta c_0}, \end{aligned} \tag{2}$$

with

$$\begin{aligned} \mathbf{L} &= \begin{bmatrix} 1+\frac{M_x^2}{\beta(1+\beta)} & \frac{M_xM_y}{\beta(1+\beta)} \\ \frac{M_xM_y}{\beta(1+\beta)} & 1+\frac{M_y^2}{\beta(1+\beta)} \end{bmatrix}, \\ \boldsymbol{M} &= \begin{bmatrix} \boldsymbol{M}_x \\ \boldsymbol{M}_y \end{bmatrix} = \begin{bmatrix} v_x/c_0 \\ v_y/c_0 \end{bmatrix}, \\ \beta &= \sqrt{1-\|\boldsymbol{M}\|^2}, \end{aligned} \tag{3}$$

where $\boldsymbol{x}'$ and t' are the spatial and time variables in the Lorentz space respectively. Using the convention $e^{+\mathrm{j}\omega t}$ and applying this transformation to Eq. (1) gives a classical Helmholtz equation in the Lorentz space:

$$(-k_0'^2 - \nabla_{\boldsymbol{x}'}^2)\phi' = f', \tag{4}$$

with

$$\begin{aligned} \phi &= \frac{1}{\beta}\phi' e^{\mathrm{j}k_0'(\boldsymbol{M}\cdot\boldsymbol{x}')}, \\ k_0' &= \frac{\omega'}{c_0}, \\ \omega' &= \frac{\omega}{\beta}. \end{aligned} \tag{5}$$

For a 2D problem defined over a rectangular computational domain, as illustrated in Fig. 1(a), Marchner et al. [7] pointed out that applying a PML technique to

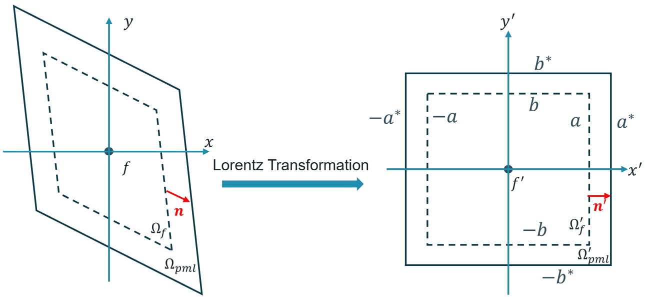

(a) In the physical space (b) In the Lorentz space

Figure 2. A 2D problem with a Mach number $M = 0.8$ and an flow angle $\theta = \pi/4$, which is a parallelogram in the physical space but a rectangle in the Lorentz space.

Eq. (4) can provide a 'stable' formulation, namely the original Lorentz model here, which writes:

$$\begin{aligned}&\left(-k_0'^2 - \gamma_x^{-1}\frac{\partial}{\partial x'}\left(\gamma_x^{-1}\frac{\partial}{\partial x'}\right)\right.\\&\left.-\gamma_y^{-1}\frac{\partial}{\partial y'}\left(\gamma_y^{-1}\frac{\partial}{\partial y'}\right)\right)\phi' = f',\end{aligned} \tag{6}$$

with

$$\gamma_i = 1 + \frac{\sigma_i}{\mathrm{j}k_0'}, \quad i = x,\ y, \tag{7}$$

where σ_i is the positive and coordinate-dependent absorbing function. It increases in the PML domain (Ω_{pml}) but vanishes in the fluid domain (Ω_f). A typical choice is the hyperbolic function:

$$\begin{aligned}\sigma_x &= \frac{\beta}{a^* - |x|},\\ \sigma_y &= \frac{\beta}{b^* - |y|}.\end{aligned} \tag{8}$$

In the classical PML theory for the Helmholtz equation [6], the absorbing function is applied along the normal direction of the interface between the fluid and the PML domains to separate the spatial coordinates. In the original Lorentz model, the absorbing function and the Helmholtz equation are not defined in the same space. In the Lorentz space, the equivalent representation of the absorbing function is:

$$\begin{aligned}\sigma_x &= \frac{\beta}{a^* - \left|\left(1 + \frac{M_x^2}{\beta(1+\beta)}\right)x' + \frac{M_xM_y}{\beta(1+\beta)}y'\right|},\\ \sigma_y &= \frac{\beta}{b^* - \left|\frac{M_xM_y}{\beta(1+\beta)}x' + \left(1 + \frac{M_y^2}{\beta(1+\beta)}\right)y'\right|}.\end{aligned} \tag{9}$$

It is noticed that in the physical space the absorbing function depends solely on either x or y, indicating that it is applied along the normal $\boldsymbol{n}$ to the interface for a rectangular domain, as illustrated in Fig. 1(a). However, in the Lorentz space, the absorbing function becomes dependent on both x' and y'. As x increases from a to a^*, the corresponding path in the Lorentz space is along the direction $\boldsymbol{n}'$, as shown in Fig. 1(b), which is no longer aligned with the normal to the interface.

Here, a modified convected Helmholtz equation with PMLs, namely the modified Lorentz model, is proposed for a 2D problem defined in Fig. 2(a), as follows:

$$\begin{aligned}&\left(-k_0'^2 - \gamma_{x'}^{-1}\frac{\partial}{\partial x'}\left(\gamma_{x'}^{-1}\frac{\partial}{\partial x'}\right)\right.\\&\left.-\gamma_{y'}^{-1}\frac{\partial}{\partial y'}\left(\gamma_{y'}^{-1}\frac{\partial}{\partial y'}\right)\right)\phi' = f'.\end{aligned} \tag{10}$$

with

$$\gamma_i = 1 + \frac{\sigma_i}{\mathrm{j}k_0'}, \quad i = x',\ y', \tag{11}$$

and

$$\begin{aligned}\sigma_{x'} &= \frac{\beta}{a^* - |x'|},\\ \sigma_{y'} &= \frac{\beta}{b^* - |y'|}.\end{aligned} \tag{12}$$

In this model, all terms are defined within the Lorentz space, where the computational domain is defined to be a rectangular region. This allows the absorbing function to be applied normal to the interface. Notably, Eq. (10) is identical to the classical Helmholtz equation with PMLs for a 2D problem shown in Fig. 2(b), so ϕ' is stable and ϕ is stable as well by using the inverse Lorentz transformation.

The main drawback of the modified Lorentz model is that it requires a rectangular domain in the Lorentz space. As a result, for different flow conditions, the computational domain in the physical space must be redefined, obtained by the inverse Lorentz transformation from a rectangular domain. In contrast, the original Lorentz model requires a rectangular domain in the physical space, independent of flow conditions. This limitation can be resolved by applying the conformal PML, which only requires a convex domain in the Lorentz space. Since any convex domain remains convex after the Lorentz transformation, the computational domain is no longer dependent on the transformation and does not need to be redefined. More details will be given in a forthcoming paper [9].

Similarly to the classical wave problem with PMLs, auxiliary variables are required to avoid the convolution integrals of ϕ' in the time domain. Following the strategy proposed by Kaltenbacher et al. [6], Eq. (10) can be rewritten as follows:

$$\begin{aligned} -\gamma_{x'}\gamma_{y'}k_0'^2\phi' - \nabla_{\boldsymbol{x}'}\cdot\boldsymbol{u}' - \nabla^2_{\boldsymbol{x}'}\phi' = f'\gamma_{x'}\gamma_{y'}, \\ \mathrm{j}k_0'\boldsymbol{u}' + \mathbf{A}\boldsymbol{u}' + \mathbf{C}\nabla_{\boldsymbol{x}'}\phi' = \mathbf{0}, \end{aligned} \tag{13}$$

with

$$\begin{aligned} \mathbf{A} = \begin{bmatrix} \sigma_{x'} & 0 \\ 0 & \sigma_{y'} \end{bmatrix}, \\ \mathbf{C} = \begin{bmatrix} \sigma_{x'} - \sigma_{y'} & 0 \\ 0 & \sigma_{y'} - \sigma_{x'} \end{bmatrix}. \end{aligned} \tag{14}$$

To get the physical results ϕ, the inverse Lorentz transformation is applied to Eqs. (13), leading to:

$$\begin{aligned} -k_0^2\phi + \frac{\mathrm{j}k_0}{\beta}\left(\alpha\phi + \boldsymbol{M}\cdot(\mathbf{L}^{-1}\nabla_{\boldsymbol{x}}\phi)\right. \\ \left.+\nabla_{\boldsymbol{x}}\cdot(\boldsymbol{M}\phi)\right) + \frac{\mathrm{j}k_0}{\beta}\boldsymbol{M}\cdot\boldsymbol{u} + \tau\phi - \\ \mathbf{L}^{-1}\nabla_{\boldsymbol{x}}\cdot(\mathbf{L}^{-1}\nabla_{\boldsymbol{x}}\phi) - \mathbf{L}^{-1}\nabla_{\boldsymbol{x}}\cdot\boldsymbol{u} = f\gamma_{x'}\gamma_{y'} \\ \frac{\mathrm{j}k_0}{\beta}\boldsymbol{u} - \frac{\mathrm{j}k_0}{\beta}\boldsymbol{M}\phi + \mathbf{A}\boldsymbol{u} + \mathbf{C}\mathbf{L}^{-1}\nabla_{\boldsymbol{x}}\phi = \mathbf{0}, \end{aligned} \tag{15}$$

with

$$\begin{aligned} \alpha = \frac{\sigma_{x'} + \sigma_{y'}}{\beta}, \\ \tau = \frac{\sigma_{x'}\sigma_{y'}}{\beta^2}. \end{aligned} \tag{16}$$

Applying the inverse Fourier transformation to Eq. (15) and implementing it in a finite element context, the modified Lorentz model can be expressed in a discrete form:

$$\begin{aligned} \begin{bmatrix} \mathbf{M}_{11} & \mathbf{0} \\ \mathbf{0} & \mathbf{0} \end{bmatrix} \begin{bmatrix} \ddot{\boldsymbol{\phi}}(t) \\ \ddot{\mathbf{u}}(t) \end{bmatrix} + \begin{bmatrix} \mathbf{D}_{11} & \mathbf{D}_{12} \\ \mathbf{D}_{21} & \mathbf{D}_{22} \end{bmatrix} \begin{bmatrix} \dot{\boldsymbol{\phi}}(t) \\ \dot{\mathbf{u}}(t) \end{bmatrix} \\ + \begin{bmatrix} \mathbf{K}_{11} & \mathbf{K}_{12} \\ \mathbf{K}_{21} & \mathbf{K}_{22} \end{bmatrix} \begin{bmatrix} \boldsymbol{\phi}(t) \\ \mathbf{u}(t) \end{bmatrix} = \begin{bmatrix} \mathbf{F}(t) \\ \mathbf{0} \end{bmatrix}, \end{aligned} \tag{17}$$

with

$$\begin{aligned} \mathbf{M}_{11} &= \int_\Omega \frac{1}{c_0^2}\mathbf{N}^T\mathbf{N}\mathrm{d}\Omega, \\ \mathbf{C}_{11} &= \frac{1}{\beta c_0}\int_\Omega \alpha\mathbf{N}^T\mathbf{N} + (\boldsymbol{M}\mathbf{N})^T\mathbf{L}^{-1}\mathbf{B} - \mathbf{B}^T\boldsymbol{M}\mathbf{N}\mathrm{d}\Omega, \\ \mathbf{K}_{11} &= \int_\Omega \tau\mathbf{N}^T\mathbf{N} + (\mathbf{L}^{-1}\mathbf{B})^T\mathbf{L}^{-1}\mathbf{B}\mathrm{d}\Omega, \\ \mathbf{D}_{12} &= \frac{1}{\beta c_0}\int_\Omega \mathbf{N}\boldsymbol{M}^T\mathbf{N}_1\mathrm{d}\Omega, \\ \mathbf{K}_{12} &= \int_\Omega (\mathbf{L}^{-1}\mathbf{B})^T\mathbf{N}_s\mathrm{d}\Omega, \\ \mathbf{D}_{21} &= \frac{1}{\beta c_0}\int_\Omega \mathbf{N}_1^T\boldsymbol{M}\mathbf{N}\mathrm{d}\Omega, \\ \mathbf{D}_{22} &= \frac{1}{\beta c_0}\int_\Omega \mathbf{N}_1^T\mathbf{N}_1\mathrm{d}\Omega, \\ \mathbf{K}_{21} &= \int_\Omega \mathbf{N}_1^T\mathbf{C}\mathbf{L}^{-1}\mathbf{B}\mathrm{d}\Omega, \\ \mathbf{K}_{22} &= \int_\Omega \mathbf{N}_1^T\mathbf{A}\mathbf{N}_1\mathrm{d}\Omega, \end{aligned} \tag{18}$$

where $\Omega = \Omega_f \cup \Omega_{pml}$, $\phi(t) := \mathbf{N}\boldsymbol{\phi}(t)$, $\boldsymbol{u}(t) := \mathbf{N}_1\mathbf{u}(t)$, $\mathbf{B}$ and $\mathbf{B}_1$ are the gradients of $\mathbf{N}$ and $\mathbf{N}_1$ respectively.

By iteratively solving Eq. (17), the wave propagation in a moving media can be dynamically simulated. However, to reduce the dispersion error and achieve reasonable accuracy, the number of elements should increase with frequency [10], making such a model difficult to run online. Additionally, in Eq. (17), auxiliary variables $\mathbf{u}(t)$ are required over the PML domain, increasing the computational burden.

3. MODEL ORDER REDUCTION

MOR has been widely studied to accelerate transient simulations by splitting the task into offline and online phases. In the offline phase, a stable and accurate ROM is created by projecting the sparse, large system matrices onto small, dense system matrices. In the online phase, the original full-order model (FOM) is replaced with a smaller ROM to perform the simulation efficiently. In the field of acoustics, the projection basis is typically generated using Krylov subspaces or proper orthogonal decomposition. However, these approaches may introduce instabilities into the ROM, necessitating special treatment to ensure stability.

In the MOR of the wave equation with PMLs, it is proven that a split projection basis can preserve stability [4]. Since Eq. (17) originates from the Helmholtz equation with PMLs in the Lorentz space (Eq. (10)), the strategy of splitting the projection basis should work as well.

Given a projection basis $\mathbf{V}$ of Eq. (17) from the Krylov subspaces or proper orthogonal decomposition, it can be expressed according to the system variables:

$$\mathbf{V} = \begin{bmatrix} \mathbf{V}_\phi \\ \mathbf{V}_{\boldsymbol{u}} \end{bmatrix}, \tag{19}$$

where $\mathbf{V}_\phi \in \mathbb{R}^{N_\phi \times r}$, $\mathbf{V}_{\boldsymbol{u}} \in \mathbb{R}^{N_{\boldsymbol{u}} \times r}$, $r \ll N_\phi + N_{\boldsymbol{u}}$, N_ϕ and $N_{\boldsymbol{u}}$ are size of variables $\phi(t)$ and $\mathbf{u}(t)$ respectively. Then, the projection basis can be split into two blocks as follows:

$$\bar{\mathbf{V}} = \begin{bmatrix} \bar{\mathbf{V}}_\phi & \mathbf{0} \\ \mathbf{0} & \bar{\mathbf{V}}_{\boldsymbol{u}} \end{bmatrix}, \tag{20}$$

where $\bar{\mathbf{V}}_\phi = orth(\mathbf{V}_\phi)$ and $\bar{\mathbf{V}}_{\boldsymbol{u}} = orth(\mathbf{V}_{\boldsymbol{u}})$. With this projection basis, the ROM of Eq. (17) is:

$$\begin{bmatrix} \mathbf{M}_{11,r} & \mathbf{0} \\ \mathbf{0} & \mathbf{0} \end{bmatrix} \begin{bmatrix} \ddot{\phi}_r(t) \\ \ddot{\mathbf{u}}_r(t) \end{bmatrix} + \begin{bmatrix} \mathbf{D}_{11,r} & \mathbf{D}_{12,r} \\ \mathbf{D}_{21,r} & \mathbf{D}_{22,r} \end{bmatrix} \begin{bmatrix} \dot{\phi}_r(t) \\ \dot{\mathbf{u}}_r(t) \end{bmatrix} + \begin{bmatrix} \mathbf{K}_{11,r} & \mathbf{K}_{12,r} \\ \mathbf{K}_{21,r} & \mathbf{K}_{22,r} \end{bmatrix} \begin{bmatrix} \phi_r(t) \\ \mathbf{u}_r(t) \end{bmatrix} = \begin{bmatrix} \mathbf{F}_r(t) \\ \mathbf{0} \end{bmatrix}, \tag{21}$$

with

$$\begin{aligned} &\mathbf{M}_{11,r} = \bar{\mathbf{V}}_\phi^T \mathbf{M}_{11} \bar{\mathbf{V}}_\phi, \mathbf{D}_{11,r} = \bar{\mathbf{V}}_\phi^T \mathbf{D}_{11} \bar{\mathbf{V}}_\phi, \\ &\mathbf{K}_{11,r} = \bar{\mathbf{V}}_\phi^T \mathbf{K}_{11} \bar{\mathbf{V}}_\phi, \mathbf{D}_{12,r} = \bar{\mathbf{V}}_\phi^T \mathbf{D}_{12} \bar{\mathbf{V}}_{\boldsymbol{u}}, \\ &\mathbf{K}_{12,r} = \bar{\mathbf{V}}_\phi^T \mathbf{K}_{12} \bar{\mathbf{V}}_{\boldsymbol{u}}, \mathbf{D}_{21,r} = \bar{\mathbf{V}}_{\boldsymbol{u}}^T \mathbf{D}_{21} \bar{\mathbf{V}}_\phi, \\ &\mathbf{K}_{21,r} = \bar{\mathbf{V}}_{\boldsymbol{u}}^T \mathbf{K}_{21} \bar{\mathbf{V}}_\phi, \mathbf{D}_{22,r} = \bar{\mathbf{V}}_{\boldsymbol{u}}^T \mathbf{D}_{22} \bar{\mathbf{V}}_{\boldsymbol{u}}, \\ &\mathbf{K}_{22,r} = \bar{\mathbf{V}}_{\boldsymbol{u}}^T \mathbf{K}_{22} \bar{\mathbf{V}}_{\boldsymbol{u}}, \mathbf{F}_r(t) = \bar{\mathbf{V}}_\phi \mathbf{F}(t), \\ &\phi(t) \approx \bar{\mathbf{V}}_\phi \phi_r(t), \mathbf{u}(t) \approx \bar{\mathbf{V}}_{\boldsymbol{u}} \mathbf{u}_r(t). \end{aligned} \tag{22}$$

With this ROM, the transient simulation of wave propagation in moving media can be performed efficiently.

4. NUMERICAL VALIDATION

In this section, the proposed formulation of the convected wave equation and its stability-preserving MOR are examined. First, the modified Lorentz formulation (Eq. (10)) is compared to the original Lorentz formulation (Eq. (6)) in the frequency domain to justify the modification. Second, stability and accuracy of the proposed ROM (Eq. (21)) are evaluated and the efficiency of the ROM is demonstrated as well.

The acoustic radiation of a monopole source is considered. Two flow angles, $\theta = 0$ and $\pi/4$, are chosen

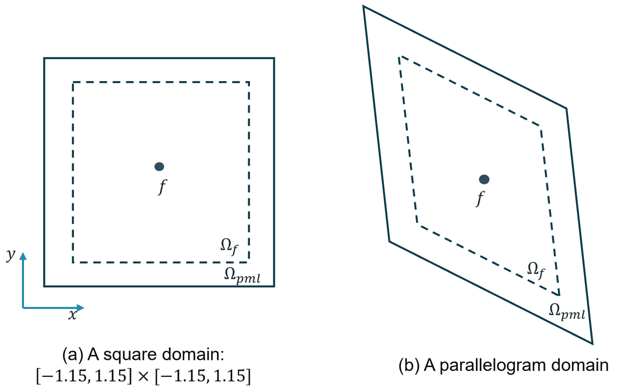

Figure 3. The computational domains in the physical space.

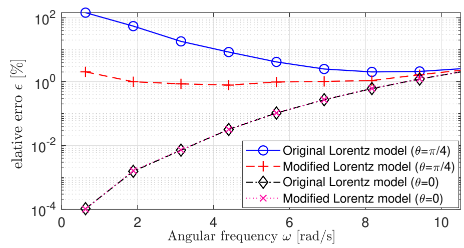

Figure 4. Relative errors as a function of the angular frequency.

with a Mach number $M = 0.8$. Consequently, two computational domains need to be considered, as illustrated in Fig. 3. The square domain is applied to two cases: the original Lorentz model with $\theta = 0$ and $\pi/4$, and the modified Lorentz model with $\theta = 0$ only. The parallelogram domain, with an area equal to that of the square domain, is used for the modified Lorentz model with $\theta = \pi/4$, which is a square after the Lorentz transformation.

The computational domains are discretized using quadrilateral elements with quadratic Lagrange shape functions. The maximum element size is set to 0.025, resulting in at least 10.7 elements per shortest wavelength, which ensures accuracy for the highest analysis frequency $\omega = 3\pi$ rad/s. Surrounding the fluid domain are six PML layers, each with the same element size as in the fluid domain. Note that the sound speed and density are both set to unity, making all quantities non-dimensional. The monopole source is located at the origin, where the mesh is locally refined by a factor of 2 to reduce numerical er-

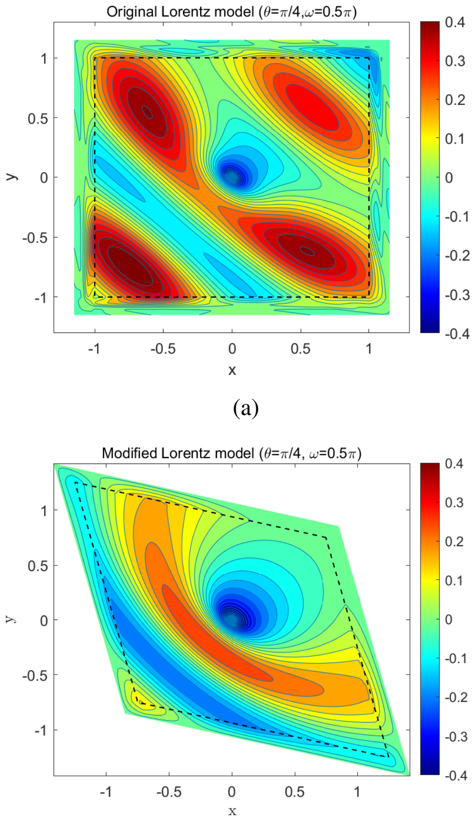

(a)

(b)

Figure 5. Real part of the numerical solution at $\theta = \pi/4$, $\omega = 0.5\pi$ rad/s and $M = 0.8$ for the original Lorentz model (a) and the modified Lorentz model (b).

rors.

4.1 Frequency domain

The relative L^2-error at each frequency is computed:

$$\epsilon(\omega) = 100\frac{\|\phi_{ex}(\omega) - \phi_{num}(\omega))\|}{\|\phi_{ex}(\omega)\|}, \tag{23}$$

where $\phi_{ex}(\omega)$ and $\phi_{num}(\omega)$ are, respectively, the exact solution and the discretized solution for all FE nodes in Ω_f, excluding the disk of radius 0.1 centered at the excitation source.

Relative errors are plotted in Fig. 4. Some findings can be made. The original Lorentz model and the modified Lorentz model show identical performance when

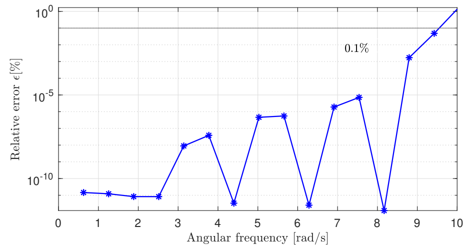

Figure 6. Relative errors as a function of the angular frequency.

$\theta = 0$, where the flow direction is along x-axis. In this case, the absorbing function is applied along the normal to the interface for both models. However, when $\theta = \pi/4$, the modified Lorentz model is more accurate than the original one, especially at low frequency, where the original Lorentz model becomes invalid.

Fig. 5 illustrates the difference between the two models at low frequency when the flow is not parallel to the x-axis. In the original Lorentz model, the wave is distorted in the PML domain, whereas in the modified Lorentz model it is perfectly absorbed.

4.2 Time domain

The modified Lorentz model is transformed into the time-domain formulation by introducing additional variables, resulting in a FOM of 57 685 degrees of freedom (DOFs). It consists of 39 174 DOFs for the acoustic potential $\phi(t)$ and 18 512 DOFs for additional variables $\boldsymbol{u}(t)$.

The Krylov subspace in combination with the AKSA algorithm [11] is run to calculate the projection basis on a personal laptop with a twelve-core 2.6 GHz processor and 32 GB of RAM. The reduction tolerance is set to 0.1% over the frequency range of interest $\omega \in [0.2\pi, 3\pi]$. Applying the split projection basis to the timed-domain model leads to a ROM of 200 DOFs. The whole MOR process requires only around 52 s.

The relative error between the frequency response functions of the FOM and the ROM is shown in Fig. 6, where the relative L^2-error is used again, defined in the same way as in Eq. (23) but with reference to the solution of the FOM. The ROM is accurate over the fluid domain within the frequency range of interest.

Fig. 7 provides the eigenvalues of the ROM, indicating its stability. The time-domain simulation is performed under the input of a Gaussian pulse with a center angular

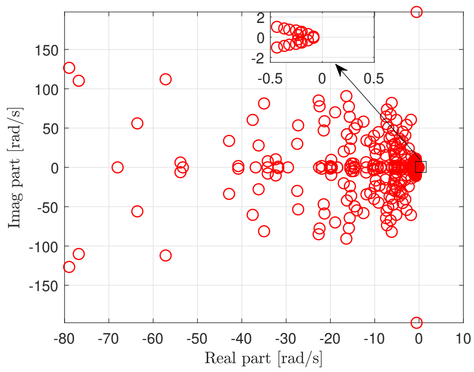

Figure 7. Eigenvalues of the ROM.

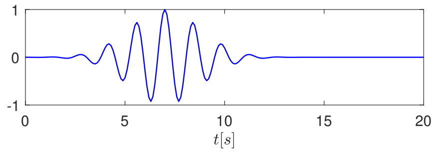

(a)

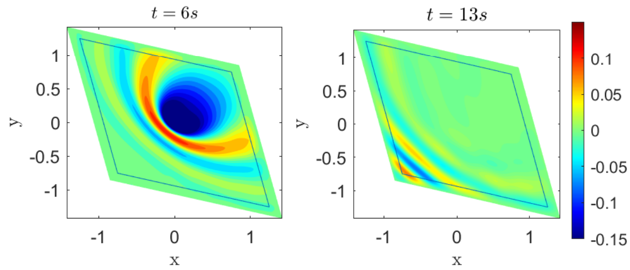

(b)

Figure 8. Time-domain simulation results: (a) Input signal and (b) snapshots of the solution at different instants

frequency $\omega = 1.4\pi$ rad/s, as plotted in Fig. 8(a). The sampling frequency is set to $10\,\mathrm{Hz}$ and the Newmark-β method is used for the time marching, where the parameters are set to $\gamma = 0.5$ and $\beta = 0.25$. The solutions at $t = 6\,\mathrm{s}$, $13\,\mathrm{s}$ are shown in Fig. 8(b). The wave is generated at the origin and is finally absorbed by the PMLs. On average, this simulation takes only $2.2 \times 10^{-4}\,\mathrm{s}$ per timestep. However, in the same setup, the FOM requires approximately $0.16\,\mathrm{s}$ per timestep.

5. CONCLUSIONS

This paper presents a method for constructing a stable ROM for the convected wave equation with perfectly matched layers (PMLs). PMLs are applied to the convected Helmholtz equation in the Lorentz space, offering greater accuracy than the existing approach by [7], which performs poorly at low frequencies. By introducing additional variables, a time-domain formulation is derived, which can retain stability in the ROM when employing the split basis in one-sided projection. Numerical experiments demonstrate that the proposed ROM remains stable, maintains accuracy, and achieves a substantial speedup in time-domain simulations compared to FOM simulations.

6. ACKNOWLEDGMENTS

The Research Foundation–Flanders (FWO) is gratefully acknowledged for its support through travel grant no. V460624N. Internal Funds KU Leuven are gratefully acknowledged for their support.

7. REFERENCES

[1] Y. Cai, S. van Ophem, W. Desmet, and E. Deckers, "Model order reduction of time-domain vibro-acoustic finite element simulations with admittance boundary conditions for virtual sensing applications," *Mechanical Systems and Signal Processing*, vol. 205, p. 110847, 2023.

[2] Y. Cai, S. van Ophem, W. Desmet, and E. Deckers, "Model order reduction of time-domain vibro-acoustic finite element simulations with non-locally reacting absorbers," *Computer Methods in Applied Mechanics and Engineering*, vol. 416, p. 116345, 2023.

[3] Y. Cai, S. van Ophem, W. Desmet, and E. Deckers, "Model order reduction of time-domain vibro-acoustic finite element simulations with poroelastic materials," *Computer Methods in Applied Mechanics and Engineering*, vol. 426, p. 116980, 2024.

[4] Y. Cai, S. van Ophem, S. Wu, W. Desmet, and E. Deckers, "Model order reduction of time-domain acoustic finite element simulations with perfectly matched layers," *Computer Methods in Applied Mechanics and Engineering*, vol. 431, p. 117298, 2024.

[5] F. Q. Hu, "A perfectly matched layer absorbing boundary condition for linearized Euler equations

with a non-uniform mean flow," *Journal of Computational Physics*, vol. 208, no. 2, pp. 469–492, 2005.

[6] B. Kaltenbacher, M. Kaltenbacher, and I. Sim, "A modified and stable version of a perfectly matched layer technique for the 3-d second order wave equation in time domain with an application to aeroacoustics," *Journal of computational physics*, vol. 235, pp. 407–422, 2013.

[7] P. Marchner, H. Beriot, X. Antoine, and C. Geuzaine, "Stable perfectly matched layers with Lorentz transformation for the convected Helmholtz equation," *Journal of Computational Physics*, vol. 433, p. 110180, 2021.

[8] E. Bécache, A. B.-B. Dhia, and G. Legendre, "Perfectly matched layers for the convected Helmholtz equation," *SIAM Journal on Numerical Analysis*, vol. 42, no. 1, pp. 409–433, 2004.

[9] Y. Cai and G. Gabard, "Model order reduction of the convected wave equation with perfectly matched layers." Manuscript in preparation, 2025.

[10] H. Bériot, G. Gabard, and E. Perrey-Debain, "Analysis of high-order finite elements for convected wave propagation," *International Journal for Numerical Methods in Engineering*, vol. 96, no. 11, pp. 665–688, 2013.

[11] A. van de Walle, *The power of model order reduction in vibroacoustics and its applications in model-based sensing*. PhD thesis, KU Leuven, 2018.